

Finite Size and Current Effects on IV Characteristics of Josephson Junction Arrays

M.V. Simkin and J.M. Kosterlitz

Department of Physics, Brown University, Providence, RI 02912, U.S.A

(June 19, 2021)

The effects of finite size and of finite current on the current-voltage characteristics of Josephson junction arrays are studied both theoretically and by numerical simulations. The cross-over from non-linear to linear behavior at low temperature is shown to be a finite size effect and the non-linear behavior at higher temperature, $T > T_{KT}$, is shown to be a finite current effect. These are argued to result from competition between the length scales characterizing the system. The importance of boundary effects is discussed and it is shown that these may dominate the behavior in small arrays.

74.25.Fy, 74.50.+r, 74.60.Jy

Two dimensional ($2D$) Josephson junction arrays (JJA) in the absence of an external magnetic field have been extensively studied [1–7] as model systems to observe the Kosterlitz-Thouless (KT) transition [8,9]. In the thermodynamic limit when the array size $N \rightarrow \infty$ and the applied current $I \rightarrow 0$ such that $IN \rightarrow \infty$ the current-voltage (IV) relation is $V \sim I^{a(T)}$ where the exponent $a(T) \geq 3$ when the temperature $T \leq T_{KT}$ and $a(T) = 1$ when $T > T_{KT}$ [10,11]. However, it is observed in experiments on small arrays [1] and in simulations [12] that the IV relation for $T < T_{KT}$ becomes linear when the applied current I is lowered below some threshold value. An explanation that this is due to a residual magnetic field inducing some free vortices was proposed [1] and an opposing point of view that this is an intrinsic effect was offered [12]. However, experiments on large arrays [5] show no cross-over to linear behavior at $T < T_{KT}$ down to the lowest accessible currents which implies that a low T linear IV relation is a finite size effect. In this article, we demonstrate both analytically and numerically that this is a finite size effect and that the nonlinear IV relation becomes linear for $I < I_x \approx I_o/N$ where I is the applied current per junction and I_o is the critical current. It is also observed that the IV relation is also non-linear at temperatures slightly above T_{KT} and we show that this is a finite current effect for $I > I_f \approx I_o/\xi_+(T)$ where $\xi_+(T)$ is the dimensionless correlation length for $T > T_{KT}$.

The behavior of the system is controlled by the length scales in the problem: the linear size N of the array, the current length $\xi_I = I_o/I$ which is the maximum size of a bound vortex pair in the presence of a current I and the thermal correlation length $\xi(T)$ which diverges as $T \rightarrow T_{KT}^+$ and is infinite for $T \leq T_{KT}$. Above T_{KT} , $\xi = \xi_+(T)$ may be interpreted as the size of the largest bound pair which is stable against thermal fluctuations, while bound pairs of all sizes exist for $T \leq T_{KT}$. The essential difference is that, for $T > T_{KT}$, there is also a finite density of thermally excited free vortices leading to a linear resistivity $R \sim \xi_+^{-2}$ while for $T < T_{KT}$ the only free vortices are due to the current unbinding of vortex pairs which leads to a non-linear IV relation. In the $2DXY$ model which describes the system, there is

a fourth length scale $\xi_-(T)$ which also diverges at T_{KT} and $\xi_+ \sim \xi_-^{2\pi}$ [13]. This length plays a rather different role to the others as it is a measure of the scale at which the renormalized vortex interaction $K(l)$ is essentially at its asymptotic value $K(\infty) = K_R(T)$. A renormalization group analysis shows that ξ_- is the scale at which deviations from critical behavior become significant and not the scale at which the RG equations become invalid. The other scales N, ξ_+, ξ_I are scales at which the RG equations do become invalid and, to proceed, some physically motivated approximation such as Debye-Hückel [14] must be made and the result extrapolated back.

A scaling assumption for the resistivity R which is consistent with the renormalization group is

$$V/I = e^{-z l} \mathcal{R}(N e^{-l}, \xi e^{-l}, \xi_I e^{-l}, l/\ln \xi_-) \quad (1)$$

where the dynamical exponent $z = 2$ and \mathcal{R} is an unknown scaling function. This scaling form is familiar from more conventional scaling functions with the exception of the combination $l/\ln \xi_-$ which is a consequence of the marginally relevant and irrelevant scaling fields in the system. The ultimate effect of this is to produce temperature and current dependent power laws. One can obtain some information from the scaling ansatz by choosing a value of l at which the scaling function \mathcal{R} can be computed. For example, in the case $\xi_I < N, \xi$, one can choose $e^l = \xi_I$ at which scale all vortex pairs are unbound by the current and the vortices may be regarded as moving independently in a viscous medium driven by the applied current so that

$$V/I = I^2 \mathcal{R}(N/\xi_I, \xi/\xi_I, 1, \ln \xi_I/\ln \xi_-) \quad (2)$$

For $T \leq T_{KT}, N \rightarrow \infty$ and $\ln \xi_I > \ln \xi_-$ we expect

$$\mathcal{R}(\infty, \infty, 1, \ln \xi_I/\ln \xi_-) \sim I^{1/\ln \xi_-(T)} \sim I^{x(T)} \quad (3)$$

where $\xi_-(T) = \exp(1/x(T))$ with $x(T) = b|T - T_{KT}|^{1/2}$, which leads to the standard nonlinear IV relation $V \sim I^{\pi K_R(T)+1}$ as the renormalized stiffness constant $\pi K_R(T) = 2 + x(T)$ and, when $\ln \xi_I < \ln \xi_-$, we expect $V \sim I^3$. Finite size dominated behavior is also contained in Eq.(1) by taking $N < \xi_I$ and $e^l = N$ to obtain

$$V/I = N^{-2}\mathcal{R}(1, \infty, \xi_I/N, \ln N/\ln \xi_I) \quad (4)$$

Now, when $\ln N > \ln \xi_-$, identical arguments lead to a linear IV relation $V/I \sim N^{-\pi K_R(T)}$ and $V/I \sim N^{-2}$ when $\ln N < \ln \xi_-$. By making appropriate assumptions about the behavior of the unknown scaling function \mathcal{R} in the various limits, all the expected behaviors can be reproduced and one expects qualitative changes when one of the ratios of lengths is of order unity. Of course, real dynamical calculations should be done to determine the functional form of \mathcal{R} at the scale l and then use the RG equations to extrapolate to physical values of the parameters. We have been unable to do this explicitly but hope to address this in the future. The strategy of this paper is to numerically simulate the IV relation and to interpret the data by these scaling considerations.

We have performed simulations on unfrustrated square $N \times N$ arrays of various sizes from $N = 4$ to $N = 64$ at different temperatures to measure the voltage across the array as a function of the external current I per bond. We use a modification of the Langevin dynamical method [6,7] as proposed by Falo, Bishop and Lomdahl [15]. We assume that all junctions have the same critical current I_o and are shunted by equal resistances R . Each superconducting grain at the vertices of the lattice has a capacitance C to ground. The dynamical equations for the phase θ_n and the voltage V_n of the superconducting grain at site n follow from charge conservation and the Josephson equation.

$$\begin{aligned} d\theta_n/dt &= 2eV_n/\hbar \\ CdV_n/dt &= I_o \sum_{\langle m \rangle} \sin(\theta_m - \theta_n) + \\ R^{-1} \sum_{\langle m \rangle} (V_m - V_n) &+ \sum_{\langle m \rangle} I_{mn}^{th} \end{aligned} \quad (5)$$

The sum over $\langle m \rangle$ is over the nearest neighbors of site n and I_{mn}^{th} is a thermal noise current in the bond mn satisfying the fluctuation dissipation relation

$$\langle I_{ij}^{th}(t) I_{kl}^{th}(t') \rangle = (2T/R)(\delta_{ik}\delta_{jl} - \delta_{il}\delta_{jk})\delta(t - t') \quad (6)$$

The capacitances C to ground are introduced purely for computational convenience and the simulations were performed with an intermediate value of the McCumber-Stewart parameter [16] $\beta = 2e^2 R^2 I_o C / \hbar = 1$.

To imitate a typical experimental configuration, we use current injection and extraction from superconducting busbars at two opposite edges of the array. The busbars are modelled by columns of N superconducting grains coupled by infinitely strong junctions, each of these grains again having a capacitance C to ground so that, in the absence of a magnetic field, the phase θ and the potential V will be the same everywhere on a bar. The busbars are each connected to the array by a set of N junctions which are assumed identical to those in the array. With this geometry, separate equations of motion are necessary for the phases θ_L, θ_R and potentials V_L, V_R

of the busbars on the left and right edges of the array. Modelling the bars in this way, they are very similar to the equations of motion for the phases and potentials of the sites in the interior of the array.

$$\begin{aligned} d\theta_L/dt &= 2eV_L/\hbar \\ d\theta_R/dt &= 2eV_R/\hbar \\ CdV_L/dt &= I + I_o N^{-1} \sum_{i=1}^N \sin(\theta_i - \theta_L) + \\ R^{-1} N^{-1} \sum_{i=1}^N (V_i - V_L) & \\ CdV_R/dt &= -I + I_o N^{-1} \sum_{i=1}^N \sin(\theta_i - \theta_R) + \\ R^{-1} N^{-1} \sum_{i=1}^N (V_i - V_R) & \end{aligned} \quad (7)$$

where I is the current per bond injected into the left busbar and extracted from the right. The sums over i are over the N sites connected to the busbars.

This busbar geometry has some advantages over the more usual method of uniform current injection where an equal current is injected or extracted from each site at the edges of the array and is not technically difficult to implement. In fact, it is easier in the presence of an external magnetic field as the gauge invariant phase is constant along the busbars and the currents in the bonds attached to them are automatically properly accounted for, in contrast to uniform injection. The potential drop across a piece of the array in the presence of an applied current is due to free vortices, which may be produced by thermal excitation, by the applied current or by an external magnetic field, being driven across the array perpendicular to the current. Uniform injection emphasizes dissipation at the edges where the current is injected and extracted as vortices are easily created there and will be attracted to the edges by their images. Unbinding of a vortex/image pair is not needed for dissipation but vortices at the edges are driven across the array by the applied current and, in a finite system, most of the dissipation may occur at the edges and not in the bulk. This implies that there is a significant voltage drop across narrow regions at the edges and that these boundary effects may dominate in finite arrays. In the busbar geometry used in the simulations reported here, vortices cannot be created adjacent to a superconducting busbar and are repelled from the array edges so that dissipation there will be suppressed. One thus expects that there will be a negligible voltage drop at the edges and all will occur in the bulk of the array. We have done simulations in both geometries to confirm this picture and find that, with the system sizes used, most of the potential drop is at the edges with uniform injection.

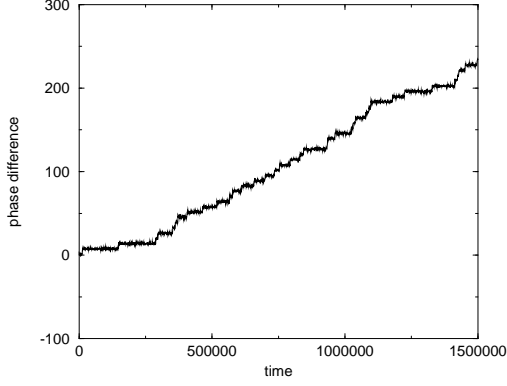


FIG. 1. Phase difference $\phi(t)$ across a $N = 32$ array at $T = 0.8$ and $I/I_o = 0.025$.

Simulations were performed on $N \times N$ square arrays in the busbar geometry with $N = 4, 8, 16, 32, 64$ at $T = 0.8, 1.0, 1.1, 1.3$ with the critical temperature $T_{KT} \approx 0.89$ [17] where T is in units of $\hbar I_o / 2e$. The equations of motion, Eqs.(5-7), were integrated using the simple Euler algorithm with a time step $\Delta t = 0.05$ in units of $1/\omega_J = (\hbar C / 2e I_o)^{1/2}$, the inverse Josephson plasma frequency. Decreasing the time step by a factor of 10 did not change the results. The system is initially in a configuration at $t = 0$ with all $\theta_n = 0 = V_n$ and integrated over at least 10^6 time steps and the phase difference $\phi(t) \equiv \theta_R(t) - \theta_L(t)$ recorded as a function of t (see Fig.1). From this, it is clear that $\phi(t)$ grows by discontinuous jumps of magnitude $2\pi n$ due to the motion of vortices. The mean voltage drop V across the system is given by

$$V/RI_o = (\phi(t_r) - \phi(0))/t_r \quad (8)$$

where t_r is the run time in units of $1/\omega_J$. To estimate the errors, we divide each run into four equal intervals and estimate V for each interval to obtain $\Delta V/V \approx 0.1$. Since the voltage V is caused by vortices crossing the array, the number n_v of these is

$$2\pi n_v = \phi(t_r) - \phi(0) \quad (9)$$

The run time t_r is chosen so that $n_v > 100$ and one expects an error in V of $\Delta V/V \approx n_v^{-1/2} \leq 0.1$ which is consistent with the estimate from block averaging.

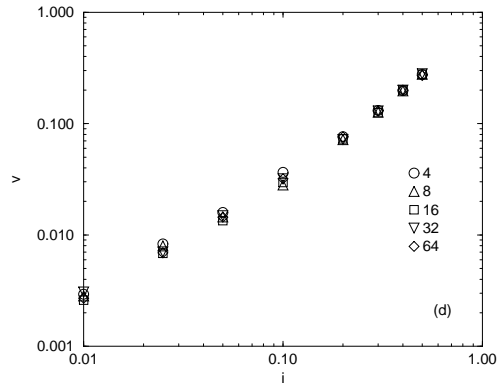
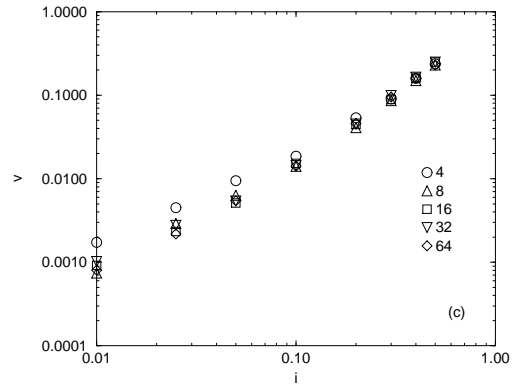
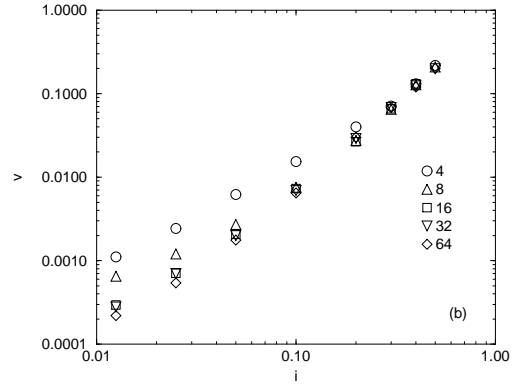
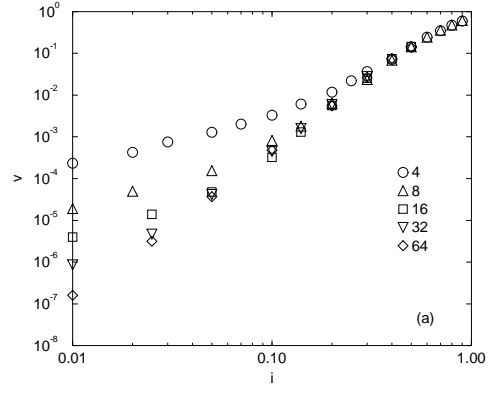


FIG. 2. IV relation ($i = I/I_0$ versus $v = V/RI_0$) with current injection from busbars for arrays of sizes $N = 4, 8, 16, 32, 64$. Errors are about the size of symbols. (a) $T = 0.8$; (b) $T = 1.0$; (c) $T = 1.1$; (d) $T = 1.3$

The results of the simulations are summarized in Figs.2(a-d) where the IV relation at fixed T is shown for several system sizes. In Fig.2(a) the data is shown for $T = 0.8 < T_{KT}$. At this temperature, we expect that ξ_- is small relative to all array sizes N and to ξ_I so that the voltage V will depend mainly on the ratio ξ_I/N and, from our scaling hypothesis of Eq.(1), we expect that $V \sim \xi_I^{-a(T)}$ when $\xi_I < N$ and $V \sim I$ when $\xi_I > N$ with a crossover between the two behaviors when $\xi_I/N = O(1)$. The data of Fig.2(a) is completely consistent with this hypothesis with the cross-over from non-linear to linear Ohmic behavior occurs at a current $I_x/I_o = 1/N$ corresponding to $\xi_I = N$. This cross-over current is in good agreement with the experimental data on small arrays: see Figs.3 and 10 of [1]. The theoretical explanation of this cross-over to Ohmic behavior at small currents at $T < T_{KT}$ is quite simple. The origin of the non-linear IV relation in $2D$ superconductors at $T < T_{KT}$ is that vortex pairs of separation $r > \xi_I = I_o/I$ are unbound by the applied current I at a rate $\sim (I/I_o)^{2\pi K_R(T)}$ and reformed at rate $\sim n_v^2$. In the steady state, these rates are equal so that $n_v \sim (I/I_o)^{\pi K_R(T)}$. Since the resistivity $V/I \propto n_v$, this yields the AHNS result [13] $V \sim I^{a(T)}$ with $a(T) = \pi K_R(T) + 1$. We note that the IV relation of Fig.2a agrees fairly well with the AHNS value for the exponent $a(T)$ at $T = 0.8$ when the theoretical estimate is $a(T) \approx 3.8$. However, our simulations are not consistent with a recent proposal that $a(T) = 2\pi K_R(T) - 1 \approx 4.5$ at $T = 0.8$ [11]. If $\xi_I > N$, no vortex pairs are unbound by the applied current as there are no pairs of separation $r > \xi_I$, so that the only source of free vortices is by thermal excitation in the finite system with $n_v \sim N^{-\pi K_R(T)}$ which yields a small linear resistivity which decreases as N increases.

When $T > T_{KT}$, the thermal length scale is $\xi_+(\tau) \approx \xi_-^{2\pi(-\tau)}$ [13] where $\tau = (T - T_{KT})/T_{KT}$ is the reduced temperature [13]. This correlation length is much larger than $\xi_-(|\tau|)$ for the same $|\tau|$ and cannot be considered small relative to ξ_I or to N for all our arrays. At very small applied currents $I/I_o < 1/\xi_+$, the system contains bound vortex pairs of separation $r < \xi_+$ and also free vortices of areal density $n_v \propto \xi_+^{-2}$. The dissipation will be dominated by these free vortices leading to a linear Ohmic IV relation with a resistivity $\propto n_v$. However, at larger currents $\xi_I < \xi_+$ the current length scale will control the dissipation and one expects a similar mechanism of vortex pair unbinding and recapture as when $\tau < 0$ leading to $V \sim I^{a(T)}$ with $1 < a(T) < 3$. These qualitative arguments imply that the crossover regime from the large current power law IV relation to the final linear Ohmic relation for small I/I_o is very wide, possibly several orders of magnitude when $T \approx T_{KT}$ and $N > \xi_+$, which is consistent with experimental observation [4,5].

The simulation results for $T > T_{KT}$ are shown in Figs.2(b),(c),(d). From these, it is clear that the cross-over from a linear to a non-linear IV relation is governed by competition between three length scales $N, \xi_I, \xi_+(T)$. For $T = 1.3$ (Fig.2d) where we expect the thermal length ξ_+ to be rather small, the IV relation is independent of the array size and the data may be interpreted by assuming $\xi_+ < N$ for all arrays and that the cross-over from non-linear to linear behavior is controlled by ξ_+/ξ_I with $\xi_+(T = 1.3) \sim 4$. At the two lower temperatures of Figs.2(b),(c), the data may be similarly interpreted with the added complication of additional finite size induced cross-overs. At $T = 1.0$, Fig.2(b) shows that the three largest systems with $N = 16, 32, 64$ start to deviate from power law behavior $V \sim I^a$ at the same current I_f , which we interpret as indicating that ξ_+/ξ_I is the controlling quantity. The two smaller arrays with $N = 4, 8$ deviate from the others when $\xi_I/N > 1$, roughly as they do when $T < T_{KT}$. We see both from numerical simulations and scaling arguments that the linear IV relation in superconducting arrays below T_{KT} for small currents is entirely due to finite size effects and the non-linear behavior above T_{KT} is a finite current effect. A consistent interpretation of the data of Figs.2(b),(c),(d) for $T > T_{KT}$ may be made and we infer that the correlation lengths $\xi_+(T) \sim 16, 8, 4$ at $T = 1.0, 1.1, 1.3$ in fair agreement with estimates from equilibrium simulations [18].

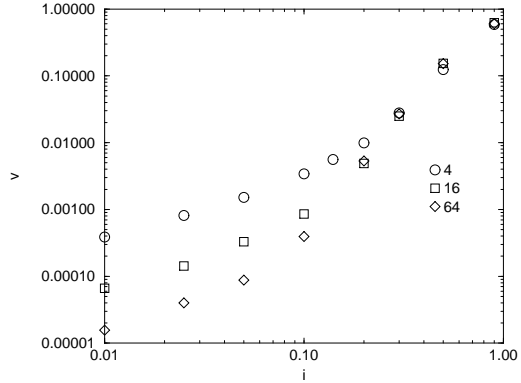


FIG. 3. IV relation ($i = I/I_0$ versus $v = V/RI_0$) with uniform current injection for sizes $N = 4, 16, 64$ at $T = 0.8$.

All the simulations discussed so far were performed in the busbar geometry and with free boundary conditions in the transverse direction to imitate the standard experimental configuration. However, several simulations have been done with uniform injection and extraction of the current and with periodic boundary conditions in the transverse direction. As discussed earlier, uniform injection is expected to emphasize dissipation at the edges of the array. To compare with current injection from busbars, we also did simulations at $T = 0.8$ with uniform injection and transverse periodic BC for three array sizes

$N = 4, 16, 64$ which are shown in Fig.3. Particularly for $N = 64$, the IV relation is linear at much larger current than for the busbar geometry which implies that there is some extra dissipation. For $N = 4$, the crossover seems to occur at about the same current as in the busbar geometry. The explanation of this is that vortices are readily nucleated at the edges as vortex/image pairs and, once created, are attracted to the edge so that much of the voltage drop or dissipation occurs not in the bulk but at the edges. This is confirmed by studying the phase profile across the array. In Fig.4(a) is shown the phase profile for injection from busbars. The phase is constant in thin layers adjacent to the bars and all the phase change occurs in the bulk. Since the voltage drop $\Delta V \propto \Delta\theta$ from Eq.(8) there is no dissipation at the edges and it is all in the bulk. On the other hand, Fig.4(b) shows the phase profile across the array for uniform injection. As expected, the major part of the phase change occurs in two thin layers at the boundaries which corresponds to motion of free vortices along the edges. This will give rise to a linear IV relation with a finite resistance which, although an edge effect which presumably is negligible in the thermodynamic limit, will dominate in a finite system at sufficiently low current.

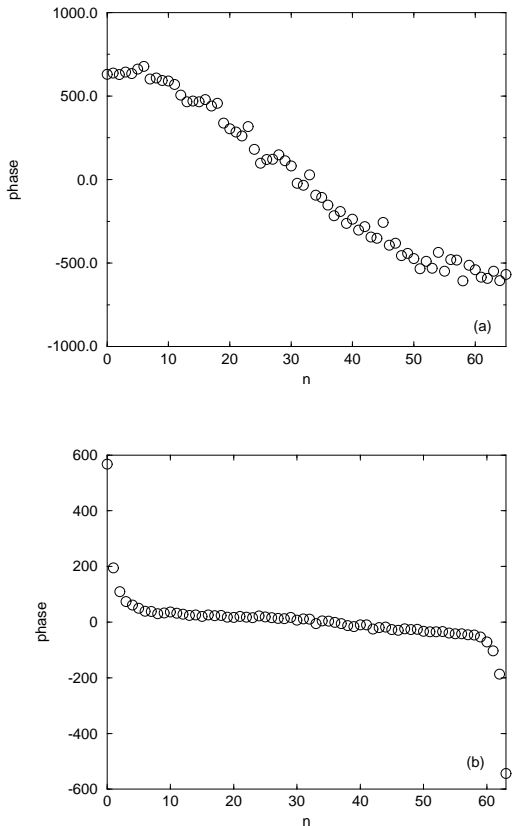


FIG. 4. Phase profile of array at time t_r . $N = 64, I/I_o = 0.05, T = 0.8$. The average phase of the grains in the n^{th} column plotted against column number n . (a)Current injection from busbars at $n = 0, 65$ with free BC in transverse direction; $t_r = 5.10^5$. (b)Uniform injection; $t_r = 2.10^5$ and periodic BC in transverse direction.

In conclusion, this work shows that experimental and simulation studies of the IV characteristics of superconducting arrays are liable to be dominated by finite size and edge effects unless great care is taken to minimize them. Large array sizes seem to be essential to make any meaningful comparison between theory and experiment or numerical simulation. When performing a DC measurement of the IV relation, dissipation at the edges should be minimized by current injection from busbars as edge effects can give a large contribution to the linear resistivity which may dominate the non-linear bulk contribution. Hopefully, this paper gives some indication how to take account of such effects and will motivate research into finding a complete scaling form for the voltage for finite size and finite currents to obtain a better understanding of the complete IV curves and not just in special limits as we do at present.

Acknowledgements: The authors are grateful to R.A. Pelcovits and J.M. Valles for invaluable conversations. This work was supported by NSF grant DMR-9222812. Computations were done at the Theoretical Physics Computing Facility at Brown University.

-
- 1 H.S.J. van der Zant, H.A. Rijken and J.E. Mooij, *J. Low Temp. Phys.* **79**, 289 (1990)
 - 2 H.S.J. van der Zant, H.A. Rijken and J.E. Mooij, *J. Low Temp. Phys.* **82**, 67 (1991)
 - 3 H.S.J. van der Zant, thesis, Delft University, (1991)
 - 4 D.J. Resnick, J.C. Garland, J.T. Boyd, S. Shoemaker and R.S. Newrock, *Phys. Rev. Lett.* **47**, 1542 (1981)
 - 5 D.W. Abraham, C.J. Lobb, M. Tinkham and T.M. Klapwijk, *Phys. Rev.* **B26**, 5268 (1982)
 - 6 K.K. Mon and S. Teitel, *Phys. Rev. Lett.* **62**, 673 (1989)
 - 7 J.S. Chung, K.H. Lee and D. Stroud, *Phys. Rev.* **B40**, 6570 (1989)
 - 8 J.M. Kosterlitz and D.J. Thouless, *J. Phys.* **C6**, 1181 (1973)
 - 9 J.M. Kosterlitz, *J. Phys.* **C7**, 1046 (1974)
 - 10 B.I. Halperin and D.R. Nelson, *J. Low Temp. Phys.* **36**, 599 (1979)
 - 11 P. Minnhagen, O. Westman, A. Jonsson and P. Olsson, *Phys. Rev. Lett.* **74**, 3672 (1994)
 - 12 S. Kim and M.Y. Choi, *Phys. Rev.* **B48**, 322 (1993)
 - 13 V. Ambegaokar, B.I. Halperin, D.R. Nelson and E.D. Siggia, *Phys. Rev.* **B21**, 1806 (1980)
 - 14 A.N. Berker and D.R. Nelson, *Phys. Rev.* **B19**, 2488 (1979)

- ¹⁵ F. Falo, A.R. Bishop and P.S. Lomdahl, Phys. Rev. B**41**, 10893 (1990)
- ¹⁶ D.E. McCumber, J. Appl. Phys. **39**, 3113 (1968); W.C. Stewart, Appl. Phys. Lett. **22**, 277 (1968)
- ¹⁷ P. Olsson, Phys. Rev. Lett. **73**, 3339 (1994)
- ¹⁸ R. Gupta and C.F. Baillie, Phys. Rev. B**45**, 2883 (1992)